JACS JOURNAL OF THE AMERICAN CHEMICAL SOCIETY

Article

Cite This: J. Am. Chem. Soc. 2020, 142, 945−952

pubs.acs.org/JACS

Nature of Excess Hydrated Proton at the Water−Air Interface

Sudipta Das,[†,§] Sho Imoto,[†,§] Shumei Sun,[†,‡] Yuki Nagata,[†] Ellen H. G. Backus,[†,‡] and Mischa Bonn*[,†]

[†]Department for Molecular Spectroscopy, Max Planck Institute for Polymer Research, Ackermannweg 10, 55128 Mainz, Germany

[‡]Department of Physical Chemistry, University of Vienna, Währinger Strasse 42, 1090 Vienna, Austria

Supporting Information

ABSTRACT: Understanding the interfacial molecular structure of acidic aqueous solutions is important in the context of, e.g., atmospheric chemistry, biophysics, and electrochemistry. The hydration of the interfacial proton is necessarily different from that in the bulk, given the lower effective density of water at the interface, but has not yet been elucidated. Here, using surface-specific vibrational spectroscopy, we probe the response of interfacial protons at the water−air interface and reveal the interfacial proton continuum. Combined with spectral calculations based on ab initio molecular dynamics simulations, the proton at the water−air interface is shown to be well-hydrated, despite the limited availability of hydration water, with both Eigen and Zundel structures coexisting at the interface. Notwithstanding the interfacial hydrated proton exhibiting bulk-like structures, a substantial interfacial stabilization by −1.3 ± 0.2 kcal/mol is observed experimentally, in good agreement with our free energy calculations. The surface propensity of the proton can be attributed to the interaction between the hydrated proton and its counterion.

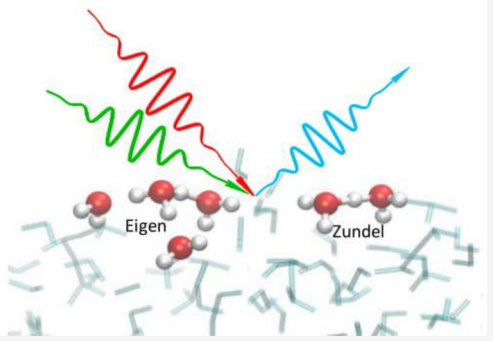

INTRODUCTION

The proton in water is as ubiquitous as water itself, given that the proton is a product of the autoionization of water ($2H_2O \rightleftharpoons H_3O^+ + OH^-$). This autoionization controls many important properties of water, e.g., allowing for charge transport in biology and electrochemistry. Through the studies of protons in bulk water, it has become evident that, much like the hydrogen-bonded network of water, the proton and its hydration shell are highly dynamic. For hydrated protons in bulk, two limiting structures, namely Zundel and Eigen, have been proposed.[1] An Eigen moiety is a proton as a part of a hydronium (H_3O^+) ion, which is solvated by three additional water molecules to produce $H_9O_4^+$. An ideal Zundel structure constitutes of a proton equally shared between two water molecules to produce the moiety $H_5O_2^+$. Static[2] and time-resolved[3−6] vibrational spectroscopy has shown that both of these moieties are present inside the bulk in their ideal and significantly distorted conformations, producing a proton continuum absorption spanning a wide vibrational frequency range, between the bend (1650 cm^{-1}) and stretch vibrations (3400 cm^{-1}) of water.

While hydrated protons in bulk have been intensely studied, less is known about protons at interfaces. Protons at interfaces are important for several systems, including atmospheric aerosols,[7] biological membranes,[8] fuel cells,[9] and electrochemical systems.[10] At the interface of acidic solutions with air, the concentration of protons at the surface is elevated compared to that in bulk.[11,12] Although the presence of the hydrated proton at the surface has been proposed from surface-specific spectroscopies, such as second harmonic generation[13] and sum-frequency generation (SFG)[14−16] as well as theoretical studies,[17−21] it is challenging to identify the SFG signatures for the Eigen and Zundel structures and the corresponding thermodynamic stability of the interfacial hydrated proton. Indeed, the energetics of interfacial proton adsorption is controversial: Voth and co-workers found, using reactive molecular dynamics simulations, that the proton is weakly attracted to the water−air interface with a free energy of 0.55 kcal/mol[22] and 1.8 kcal/mol[23] for different proton models (multistate empirical valence bond models 3.2 and 3.0, respectively). Buch and co-workers have concluded the proton to be strongly adsorbed at the surface with a free energy of ∼3 kcal/mol with a mixed quantum/classical approach.[24] Furthermore, the continuum model calculation predicts the free energy barrier of 1.3 kcal/mol.[25] Thus, both experiments and theory consistently predict a clear affinity for the hydrated proton to the surface, but the degree of reported surface affinity is rather scattered. Clearly, the free energy of adsorption is intricately connected to the structure of the interfacial hydrated proton, and an experimental verification of both structure and free energy of adsorption is therefore very desirable.

The surface activity of the hydrated proton has been considered as the limiting case of the hydronium ion. The hydronium ion has been predicted to sit on the surface with its

Received: October 8, 2019
Published: December 21, 2019

DOI: 10.1021/jacs.9b10807
J. Am. Chem. Soc. 2020, 142, 945−952

three OH groups pointing down toward the bulk, with the lone pair pointing toward the vapor phase,[17−19,22] which would point to the interfacial hydrated proton being present at the interface purely as an Eigen state. The excess proton is presumably expelled to the surface as it behaves as a defect of the hydrogen bond network.[21,26,27]

In order to address the structure of the interfacial hydrated proton, we use surface-specific vibrational spectroscopy, i.e., conventional and phase-sensitive (PS-) sum-frequency generation (SFG) spectroscopy, at the water−air interface in the presence of HCl. From our experiments, we find that the protons indeed adsorb at the surface and produce a "proton continuum" response reminiscent of that observed in bulk infrared spectroscopy. By comparing the observed experimental response with calculations, we find that the spectral response can be accounted for by the coexistence of the Eigen and the Zundel forms of interfacial solvated protons. We quantify the adsorption free energy of the proton at the surface to be ∼1.3 kcal/mol, substantially higher than k_BT of ∼0.6 kcal/mol.

RESULTS AND DISCUSSION

Figure 1a shows the SFG intensity spectra for pure H_2O, and H_2O containing 1 M HCl in the subphase. Each spectrum has a sharp response centered at ∼3700 cm^{-1} (shaded in blue), a broad response with a dual peak feature extending from ∼3000 cm^{-1} to ∼3600 cm^{-1} (shaded red), a broad featureless response spanning the range from ∼2000 to ∼3000 cm^{-1} (shaded green) and a peak at ∼1650 cm^{-1}. The sharp response at ∼3700 cm^{-1} (blue region) originates from the vibration of non-hydrogen-bonded OH groups from water pointing into the air. The broad response with a dual peak feature (red region) is the vibrational signature of hydrogen-bonded H_2O molecules at the H_2O−air interface. Vibrational coupling between hydrogen-bonded O−H groups causes the dual-peak line shape.[28] The flat featureless response in the green region for pure water is generally considered to be a nonresonant response of the interfacial water molecules (see also Supporting Information (SI), Figure S1).[29] The peak at ∼1650 cm^{-1} is the bend vibrational response of the water molecules.[30−32] In the presence of 1 M HCl, the intensity rises throughout the ∼1600−3600 cm^{-1} region and decreases around 3700 cm^{-1}. Both observations evidence interfacial proton propensity: hydronium ions—in whatever hydrated form—at the interface displace the free OH groups, enhancing the SFG signal in the hydrogen-bonded region and reducing the free OH peak intensity. The presence of 1 M NaCl does not significantly affect the surface water spectrum (Figure S2) so that it is apparent that the signal changes are primarily due to the proton. The SFG intensity changes observed both on- and off-resonance of the O−H stretch for 1 M HCl solution is not—or only very weakly—observed for NaOH,[16] NaI and NaCl[33] solutions of comparable molarity.

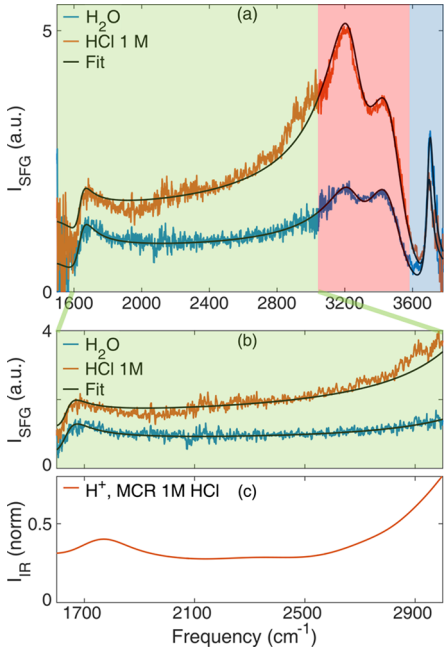

Figure 1. (a) SFG intensity at the water−air interface for pure H_2O, and H_2O containing 1 M HCl in the subphase. The black lines are fits (see SI). (b) Zoom-in of the 1600−3000 cm^{-1} region of the SFG response from pure H_2O and 1 M HCl solution. (c) Contribution to the bulk IR absorption spectrum from the hydronium ion obtained from multivariate curve resolution (MCR) analysis. The IR-MCR data are reproduced from ref 2.

Figure 1b shows the SFG intensity in the ∼1600−3000 cm^{-1} region, illustrating the enhancement of intensity in this region as a result of the presence of protons. This observation is reminiscent of the so-called proton continuum absorption in bulk acid solution, exemplified in Figure 1c. This figure shows the proton-related IR absorption in HCl solution, obtained using a multivariate curve resolution (MCR) analysis.[2] The Raman MCR signal has been shown to have a similar shape.[2]

The proton-induced increase in the 1600−3000 cm^{-1} SFG intensity clearly shows that the proton is surface active, yet the signal increase can be due to (i) OH groups of a surface-adsorbed hydrated proton (i.e., an interfacial proton continuum response); (ii) an enhanced orientation of water; or (iii) a result of the presence of charge at the surface, giving rise to a bulk contribution.[34] To address these, one needs to examine the contributions to the SFG spectra quantitatively, beyond the qualitative discussion. It is challenging to distinguish these different possible contributions from the SFG intensity spectra, because SFG intensity spectra, being proportional to the absolute square of the response function ($\chi^{(2)}$), are not quantitative: $I_{SFG} \propto |\chi^{(2)}|^2$. This means that the real (Re) and an imaginary (Im) components of $\chi^{(2)}$ cannot be disentangled. In particular, $\mathrm{Im}[\chi^{(2)}]$ directly reflects the response and orientation of interfacial molecules. PS-SFG measurement allows for direct access to the real and imaginary parts of $\chi^{(2)}$.[14,35,36]

To shed more light on the origin of the proton signal, we have performed PS-SFG measurements. Figure 2a shows $\mathrm{Im}[\chi^{(2)}]$ responses as a function of frequency at the water−air interface of pure H_2O and H_2O containing 1 M NaCl. The presence of NaCl has little effect on the response. For H_2O containing 1 M HCl, the response is enhanced and frequency-shifted. To check for a possible bulk ($\chi^{(3)}$-) contribution[34] to the enhanced response, we added 1 M NaCl to the 1 M HCl solution. The resulting doubling of the ionic strength of the solution will result in a stronger screening of the charge of the interfacial protons, reducing the Debye screening length from ∼3 to ∼2 Å. Yet, the addition of NaCl does not affect the $\mathrm{Im}[\chi^{(2)}]$ response (red dotted line), indicating that the $\chi^{(3)}$ effect does not dominate the proton-induced response of the acidic water surface.

DOI: 10.1021/jacs.9b10807
J. Am. Chem. Soc. 2020, 142, 945−952

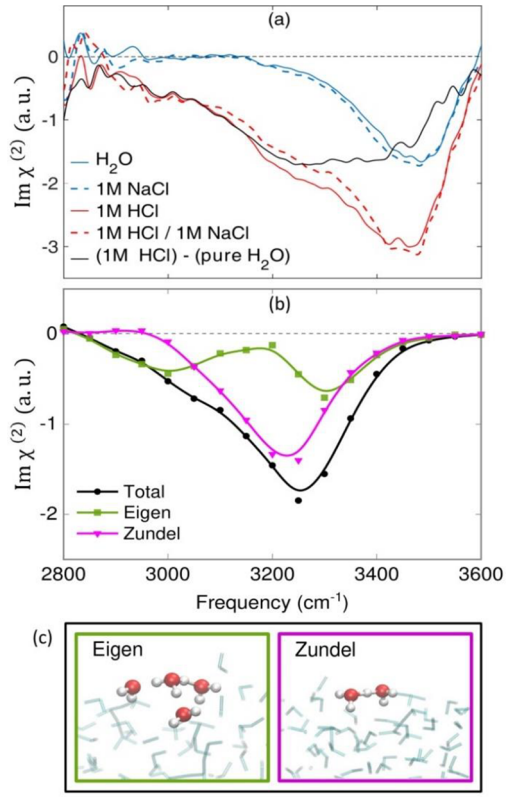

Figure 2. (a) Experimentally determined imaginary part of $\chi^{(2)}$ spectra at the H_2O–air interface for pure H_2O and in the presence of 1 M NaCl, 1 M HCl, and a solution containing both 1 M NaCl and 1 M HCl in the subphase. The black line shows the difference spectrum between the presence and absence of 1 M HCl. (b) Simulated contributions from Eigen (green) and Zundel (purple) moieties to the total (black) imaginary $\chi^{(2)}$ response of 1 M HCl. The thick lines are spline fits to the data points. Panel (c) shows the interfacial Eigen and Zundel structures. The reasonable agreement between the experimental and simulated black lines indicates the presence of both Eigen and Zundel moieties at the surface.

A clear difference exists between the shapes of the interfacial proton continuum in the intensity vs the imaginary spectrum. In the imaginary spectrum, the interfacial proton continuum appears largely above ~2800 cm^{-1}, whereas in the intensity spectrum there is also enhanced intensity below 2800 cm^{-1}, which must originate from the real part of the susceptibility, as indeed apparent from Figure S3. This low-frequency intensity increase is the direct result of the very broad interfacial proton resonance in the 2800–3500 cm^{-1} region. The observation that, at lower frequencies, the intensity is largely due to the real part of the response can be traced to the real part decaying with $\sim 1/(\nu - \nu_{res})$, away from the resonance frequency ν_{res}, whereas the imaginary part decays more quickly as $\sim 1/(\nu - \nu_{res})^2$. Thus, the response of the hydrated proton at the interface is spectrally more narrow compared to the proton continuum in the bulk. We attribute this difference to the reduced hydration of the proton at the surface (see below).

We cannot experimentally distinguish between the contributions to the signal from (i) the hydronium O–H groups and (ii) the increased orientation of water molecules with their H atoms pointing toward the bulk due to the accumulation of protons at the surface. Since overall contributions to the $\mathrm{Im}[\chi^{(2)}]$ spectra are additive, we consider the difference spectrum of 1 M HCl and pure H_2O as the "effective" $\chi^{(2)}$ response of the adsorbed protons at the surface. We note that this is a rather crude approximation: it assumes—in line with the unchanged signal upon addition of 1 M NaCl—(i) a vanishingly small $\chi^{(3)}$-bulk contributions to the signal and (ii) that the increase in downward water orientation due to the presence of protons is exactly counteracted by the displacement of interfacial water by hydronium ions. The difference spectrum (black line in Figure 2a) is broad (width ~450 cm^{-1}) and asymmetric, with intensity ranging from 2800 to 3600 cm^{-1}, i.e. well beyond the water response that peaked at 3500 cm^{-1} (width 200 cm^{-1}, blue lines), suggesting the appearance of new vibrational modes. We assign this broad proton-induced spectrum primarily to the proton at the interface. While this general shape is reminiscent of the proton continuum previously reported in bulk,[2,3] the interfacial proton continuum approaches zero at a higher frequency than that in the bulk.

To further investigate the nature of the proton at the surface, we compare the experimentally obtained spectrum with that simulated from the *ab initio* molecular dynamics (AIMD) trajectories for the air–aqueous HCl solution interface. The reactive nature of the proton transfer process is automatically captured with AIMD simulation methods, where the electronic degrees of freedom are treated explicitly.[37,38] Figure 2b and 2c show the simulated contributions of the Eigen and Zundel moieties to the $\mathrm{Im}[\chi^{(2)}]$ SFG response, and the corresponding interfacial structures, respectively. The Eigen and Zundel contributions to the spectra differ significantly. The Eigen structure shows two negative peaks: the O–H stretch peaks centered at 2950 and 3300 cm^{-1} arising from the H_3O^+ ion itself and the surrounding 3 H_2O molecules, respectively. For the Eigen conformation, the excess covalent O–H bonds of the H_3O^+ ion weaken the intramolecular O–H bonds, lowering its O–H stretch frequency. For the Zundel structure, an excess proton also weakens slightly an O–H covalent bond compared to the case of a water molecule, while the effect of the excess proton on the weakening of the O–H covalent bond is limited because an excess proton is shared by the two water molecules. As such, the O–H covalent bonds are stronger than those in H_3O^+. Interestingly, the relatively large width of the proton responses reported here contrasts the proton response reported at a lower frequency at the surface of a negative surfactant.[39]

The sum of these contributions generate one apparent peak around 3300 cm^{-1} with a very broad shoulder in the frequency range 2900–3200 cm^{-1}. The shape of the simulated overall $\mathrm{Im}[\chi^{(2)}]$ response comprising the sum of the Eigen and Zundel moieties (black spectrum in Figure 2b) agrees well with the differential $\mathrm{Im}[\chi^{(2)}]$ response of the H_2O–air interface and HCl solution–air interface determined experimentally (the black line spectrum in Figure 2a). This indicates that both Eigen and Zundel moieties are present at the surface, and our results indicate their presence in similar quantities (see Supporting Information). A precise quantification of the relative occurrence of Zundel and Eigen structures at the interface would require the inclusion of nuclear quantum effects.[40,41]

Having established reasonable agreement between theory and experiment, we can proceed to investigate how strongly the proton binds to the surface. In other words, what is the free energy of adsorption for protons to the surface? Previous theoretical reports have predicted both weak binding[21,22] (binding strength, $\Delta E_{bind} \leq 0.6$ kcal/mol) and strong binding[20,24,25,42,43] ($\Delta E_{bind} > 0.6$ kcal/mol).

DOI: 10.1021/jacs.9b10807
J. Am. Chem. Soc. 2020, 142, 945–952

To determine the value experimentally, we have monitored the SFG intensity from a D_2O–air interface as a function of the D_3O^+ to Na^+ concentration ratio at a total bulk concentration of 1 M, i.e. at constant ionic strength. We used D_2O instead of H_2O to avoid any uncertainty due to the absorbance of IR intensity by the water vapor in the air at the free OH region (~3700 cm^{-1}). We focus on the free OD intensity to quantify the surface propensity of protons at the D_2O–air interface since the free OD intensity does not suffer from potential complications due to vibrational coupling and bulk contributions to the signal and thereby provides the most direct measure for the proton density in the topmost layer of water. Figure 3a represents the SFG intensity at the D_2O–air interface containing NaCl and DCl in different concentration ratios in the subphase. The SFG intensity in the presence of 1 M NaCl (dark blue) does not significantly differ from that of pure D_2O (red). The intensity of the hydrogen-bonded region (~2200–2650 cm^{-1}) increases with increasing acid fraction in the subphase, consistent with the results for H_2O. The intensity of the free OD groups decreases with increasing concentration of acid indicating a displacement of free ODs by the adsorbed hydrated protons, again in line with the H_2O results.

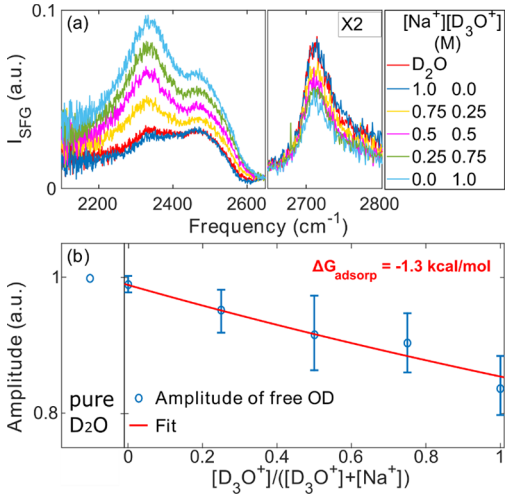

Figure 3. (a) SFG response at D_2O–air interface for pure D_2O and D_2O containing NaCl and DCl at different concentration ratios averaged over three separate experiments. (b) Amplitude associated with the "free" OD vibrations (a direct measure of the surface density) as a function of the relative concentration of D_3O^+ to Na^+ in the subphase. The data are normalized to the free OD response of pure D_2O (left data point). The red line is the fit obtained with eq 2. Error bars denote variation among three different measurement sets.

In order to gain the information on the amplitude of the free OD response, we describe the data obtained in the individual experiments separately with a Lorentzian line shape model, using a global description of each data set. Figure 3b represents the amplitude of the free OD peak as a function of the fraction of D_3O^+ to the total cation concentration in the solution. Since the total ionic strength of the solution is 1 M, the fraction of D_3O^+ in Figure 3b equals its absolute bulk concentration. The fit results show that the number of free OD groups decreases by up to ~15% in the presence of 1 M acid in the subphase.

We verified, using polarization-resolved SFG experiments,[44−46] that this reduction arises solely from the decrease in the number of free OD groups through displacement by the hydronium moieties, and not because of the change in the angular distribution of free OD groups with respect to the surface normal (see Supporting Information).[46] This is consistent with our AIMD data (see Supporting Information). Therefore, the reduction of the amplitude of the free OD band (ΔA_{freeOD}) can be directly related to the interfacial proton concentration $N^{\text{Surf}}_{D_3O^+}$:

$$N^{\text{Surf}}_{D_3O^+} \propto \Delta A_{\text{freeOD}} \tag{1}$$

In order to determine the proton adsorption free energy, we relate the adsorption free energy of interfacial proton adsorption ΔG_{ads} to $N^{\text{Surf}}_{D_3O^+}$, through ΔA_{freeOD}. In line with ref 47, the surface concentration of hydronium is obtained by describing ΔA_{freeOD} as a function of D_3O^+ concentration $C_{D_3O^+}$with the Langmuir isotherm:

$$\Delta A_{\text{freeOD}} = A^{D_2O}_{\text{freeOD}}\left(1 - \frac{C_{D_3O^+}}{C_{D_3O^+} + C_{\text{water}}e^{\Delta G_{\text{ads}}/RT}}\right) \tag{2}$$

where T is the temperature of the system. Here, $A^{D_2O}_{\text{freeOD}}$ is the amplitude of the free OD band in absence of protons, $C_{D_3O^+}$ and C_{water} are the bulk concentrations of hydronium and water respectively, and ΔG_{ads} is the Gibbs free energy of adsorption of hydronium to the surface. In this equation, we assume that all free OD intensity is gone when the surface is fully covered with hydrated protons. The model describes the data well assuming an adsorption free energy of −1.3 ± 0.2 kcal/mol (red line in Figure 3b) indicating strong adsorption of the hydrated proton.

Using the simulated density profiles (see Supporting Information) we calculated the potential of mean force, reflecting the free energy of adsorbed hydrated protons. To identify the surface, we used both the instantaneous and the average liquid interface description.[48,49] The resulting free energy profiles of the hydrated proton are shown in Figure 4a and b. The simulation results reveal a large difference in the free energy profiles; for the averaged interface description, an adsorption free energy of ~0.5 kcal/mol is found, consistent with the value of 0.55 ± 0.25 kcal/mol obtained from a previous reactive MD simulation.[22] Yet, the instantaneous interface gives a value of 1.0 ± 0.2 kcal/mol at the revPBE-D3 level of theory. The difference of the PMF with different interface descriptions has previously been reported.[21,22,50]

To unveil the difference of the free energy values for different descriptions, we computed the depth profile of the water molecules with a free O–D group which was focused on the SFG measurement by using the instantaneous and averaged interface descriptions. This free O–D group is defined using the geometrical relation of water molecules.[51] Figure 4c shows that the depth profile within the instantaneous interface description shows a very sharp distribution of water molecules with the free O–D group, while the average interface description shows an excessive broadening due to the surface nanoroughnes.[52] As such, the topmost layer of water where a water molecule with a free O–D group is located can be properly captured within the instantaneous liquid interface description.

Here, a question is how such a hydrated proton can be stable at the water–air interface. The role of the counterion for stabilizing the H_3O^+ ion has been argued.[53−55] To examine the correlation effect of these ions, we computed the radial

DOI: 10.1021/jacs.9b10807
J. Am. Chem. Soc. 2020, 142, 945−952

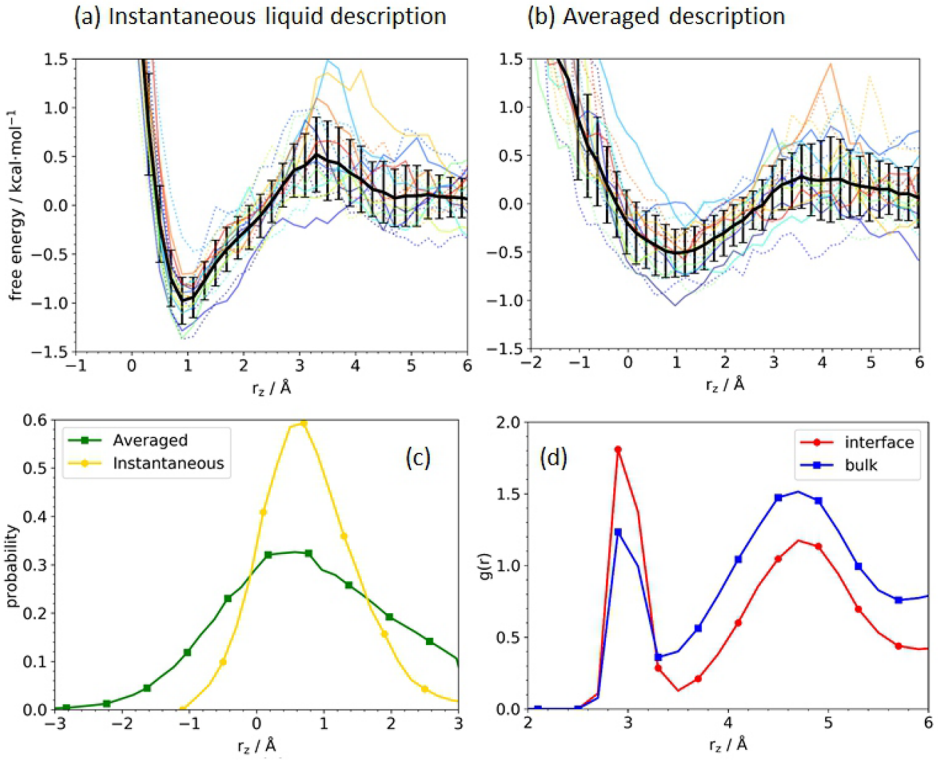

Figure 4. Simulated free energy profiles computed by using (a) averaged interface description and (b) instantaneous liquid interface description. The error bars represent the standard deviation. A total of 20 colored data sets show the profiles obtained from individual trajectories. The solid and dotted lines represent two types of water−air interface in the slab model. The average of the free energy in the range of 6 Å < $|r_z - r_G|$ < 9 Å was set to zero. (c) Simulated density profiles for instantaneous and average interface descriptions of the oxygen atoms associated with the free OD groups. (d) Radial distribution functions between the oxygen atom of H_3O^+ and Cl^- ion at the surface and in bulk. Only oxygen atoms which are in the range of $|r_z - r_G|$ < 3.11 Å are considered for surface, whereas oxygen atoms in the range of $|r_z|$ < 3.11 Å are used for bulk.

distribution functions for the H_3O^+ ion and Cl^-. The data are displayed in Figure 4d. This shows that Cl^- tends to be located next to the H_3O^+ ion, further stabilizing the H_3O^+ species at the surface compared with in bulk. This clearly indicates that the counterions Cl^- and H_3O^+ are highly correlated at the water−air interface. This is consistent with the previous studies.[53]

CONCLUSION

We have characterized the nature of the hydrated proton adsorbed at the water−air interface. Our experimental data, together with theoretical calculations, are consistent with the coexistence of the Eigen and Zundel moieties of the interfacial proton. We experimentally find that the adsorption free energy of the proton of ∼1.3 kcal/mol at the water−air interface is substantially larger than 0.6 kcal/mol (k_BT) at room temperature, implying strong surface adsorption.

EXPERIMENTAL METHODS

SFG Measurements. In conventional SFG spectroscopy, an infrared (IR) laser pulse was spatiotemporally overlapped with an 800 nm pulse at the sample surface and the reflected sum-frequency response was detected. We used a mode-locked Ti:sapphire laser (Mai Tai SP, Spectra-Physics) and a regenerative amplifier (Spitfire Ace, Spectra-Physics) pumped with a Nd:YLF laser (Empower 45, Spectra-Physics). The amplifier produces 800 nm pulses with 4.5 mJ power and an ∼45 fs pulse width, at a 1 kHz repetition rate. From its output, ∼1.7 mJ are used to pump a commercial OPA (TOPAS-C, Light Conversion) that mixes signal and idler in a $AgGaAs_2$ to crystal and produces tunable broad-band IR pulses. The IR pulses have a full width at half-maximum (fwhm) of 450 cm^{-1} and an ∼5 μJ pulse energy. The remainder of the amplifier output is spectrally narrowed to 15 cm^{-1} fwhm using a Fabry−Perot etalon (SLS Optics Ltd.). The output energy is ∼20 μJ. The diameter of the beams focused onto the samples is 0.1−0.2 mm. The incident angles for the IR and visible (800 nm) beams are 36° and 34°, respectively. The signal is collected by a spectrograph (Acton, Princeton instruments) and detected with an electron-multiplying charge-coupled device (EM-CCD) camera (Newton, Andor instruments). The acquisition time is typically 5 to 10 min depending on the signal strength. All spectra in the presented work are collected in SSP polarization (S: SFG, S: visible, P: IR), unless otherwise noted. The data are normalized by the nonresonant signal from z-cut quartz.

In the PS-SFG setup the IR and VIS beams are first focused onto y-cut quartz to create the local oscillator. Subsequently, the transmitted beams are refocused onto the sample surface using a concave mirror. The LO is passed through a delay plate to introduce a time delay relative to that of sample SFG. The angles of incidence of the IR and visible beams are 47° and 62°, respectively. See more details in ref 56.

Simulation Protocols. AIMD simulations were carried out by using the CP2K software package.[57] We used a triple-ζ quality TZV2P basis set and a charge density cutoff of 320 Ry for the plane wave. We employed the revised PBE functional (revPBE[58]) combined with Grimme's empirical dispersion D3(0) correction.[59] The choice of these calculation methods arises from the recent evaluation of the description of the interfacial water where we concluded that the revBPE-D3(0) nicely reproduces the properties of bulk and surface water among the generalized gradient approximation level of theory.[60] The simulation cell of 16.3 Å × 16.3 Å × 44.1 Å contained 10 H^+ and Cl^- ion pairs together with 160 water molecules. We obtained a total of 10 × 50 ps trajectories, which were used for analyzing the structure of the interface and compute the SFG signal. For classifying the

DOI: 10.1021/jacs.9b10807
J. Am. Chem. Soc. 2020, 142, 945−952

Zundel and Eigne structures, we used the definition of $\delta > 0.3$ for Eigen and $\delta < 0.1$ for Zundel.[1]

For the SFG spectra calculation, we used the formula[61]

$$\chi^{(2)}_{ssp}(\omega) \propto \sum_i \left\{ \left(\frac{\partial M_z}{\partial Q_i} \right) \left(\frac{\partial A_{xx}}{\partial Q_i} \right) + \left(\frac{\partial M_z}{\partial Q_i} \right) \left(\frac{\partial A_{yy}}{\partial Q_i} \right) \right\} \delta(\omega - \omega_i) \tag{3}$$

where $\left(\frac{\partial M_z}{\partial Q_i}\right)$ and $\left(\frac{\partial A_{xx}}{\partial Q_i}\right)$ denote the z-component of the transition dipole moment and the xx-element of the transition polarizability of the system with respect to the normal mode Q_i, respectively. The normal mode calculations were performed by using the revPBE-D3/aug-cc-pVDZ level theory with the ORCA quantum chemistry package.[62] The free energy landscape (potential of mean force, PMF) was computed from the density profile $\rho(r)$ via

$$\mathrm{PMF}(r) = -kT \ln\left(\frac{\rho(r)}{\rho_0} \right) \tag{4}$$

where ρ_0 is the simulated bulk water density. The simulation details are given in the Supporting Information.

■ ASSOCIATED CONTENT

Supporting Information

The Supporting Information is available free of charge at https://pubs.acs.org/doi/10.1021/jacs.9b10807.

Nonresonant SFG response; comparison of neat H_2O and 1 M NaCl; fitting procedure; the phase of the interfacial proton-continuum; angular distribution of the orientation of the "free" OD; fits and reproducibility of free OD intensity variation with varying proton concentration; computational protocol for ab initio molecular dynamics simulation; definition of interface; computational protocols for SFG spectra; sensitivity check of the Eigen/Zundel definition to SFG spectra; simulated free O−D group; hydration structure of H_3O^+ ion; proton dynamics at interfaces; additional simulation data (PDF)

■ AUTHOR INFORMATION

Corresponding Author

*bonn@mpip-mainz.mpg.de

ORCID

Yuki Nagata: 0000-0001-9727-6641

Ellen H. G. Backus: 0000-0002-6202-0280

Mischa Bonn: 0000-0001-6851-8453

Author Contributions

§S.D. and S.I. contributed equally.

Notes

The authors declare no competing financial interest.

■ ACKNOWLEDGMENTS

The authors are grateful to Maksim Grechko and Johannes Hunger for critical reading of the manuscript. This work is funded by the Deutsche Forschungsgemeinschaft (DFG, German Research Foundation) - BA 5008/3 and the MaxWater initiative from the Max Planck Society.

■ REFERENCES

(1) Marx, D. Proton transfer 200 years after von Grotthuss: Insights from ab initio simulations. *ChemPhysChem* **2006**, *7* (9), 1848−1870.

(2) Daly, C. A.; Streacker, L. M.; Sun, Y.; Pattenaude, S. R.; Hassanali, A. A.; Petersen, P. B.; Corcelli, S. A.; Ben-Amotz, D. Decomposition of the Experimental Raman and Infrared Spectra of Acidic Water into Proton, Special Pair, and Counterion Contributions. *J. Phys. Chem. Lett.* **2017**, *8* (21), 5246−5252.

(3) Thämer, M.; De Marco, L.; Ramasesha, K.; Mandal, A.; Tokmakoff, A. Ultrafast 2D IR spectroscopy of the excess proton in liquid water. *Science* **2015**, *350* (6256), 78−82.

(4) Woutersen, S.; Bakker, H. J. Ultrafast Vibrational and Structural Dynamics of the Proton in Liquid Water. *Phys. Rev. Lett.* **2006**, *96* (13), 138305.

(5) Dahms, F.; Fingerhut, B. P.; Nibbering, E. T. J.; Pines, E.; Elsaesser, T. Large-amplitude transfer motion of hydrated excess protons mapped by ultrafast 2D IR spectroscopy. *Science* **2017**, *357* (6350), 491−495.

(6) Fournier, J. A.; Carpenter, W. B.; Lewis, N. H.; Tokmakoff, A. Broadband 2D IR spectroscopy reveals dominant asymmetric $H_5O_2^+$ proton hydration structures in acid solutions. *Nat. Chem.* **2018**, *10* (9), 932−937.

(7) Roberts, J. M.; Osthoff, H. D.; Brown, S. S.; Ravishankara, A. R. N_2O_5 Oxidizes Chloride to Cl_2 in Acidic Atmospheric Aerosol. *Science* **2008**, *321* (5892), 1059−1059a.

(8) Angelova, M. I.; Bitbol, A.-F.; Seigneuret, M.; Staneva, G.; Kodama, A.; Sakuma, Y.; Kawakatsu, T.; Imai, M.; Puff, N. pH sensing by lipids in membranes: The fundamentals of pH-driven migration, polarization and deformations of lipid bilayer assemblies. *Biochim. Biophys. Acta, Biomembr.* **2018**, *1860* (10), 2042−2063.

(9) Rees, N. V.; Compton, R. G. Sustainable energy: a review of formic acid electrochemical fuel cells. *J. Solid State Electrochem.* **2011**, *15* (10), 2095−2100.

(10) Wan, K.; Yu, Z.-p.; Li, X.-h.; Liu, M.-y.; Yang, G.; Piao, J.-h.; Liang, Z.-x. pH Effect on Electrochemistry of Nitrogen-Doped Carbon Catalyst for Oxygen Reduction Reaction. *ACS Catal.* **2015**, *5* (7), 4325−4332.

(11) Mamatkulov, S. I.; Allolio, C.; Netz, R. R.; Bonthuis, D. J. Orientation-Induced Adsorption of Hydrated Protons at the Air−Water Interface. *Angew. Chem., Int. Ed.* **2017**, *56* (50), 15846−15851.

(12) Ishiyama, T.; Morita, A. Molecular dynamics analysis of interfacial structures and sum frequency generation spectra of aqueous hydrogen halide solutions. *J. Phys. Chem. A* **2007**, *111* (38), 9277−9285.

(13) Petersen, P. B.; Saykally, R. J. Evidence for an Enhanced Hydronium Concentration at the Liquid Water Surface. *J. Phys. Chem. B* **2005**, *109* (16), 7976−7980.

(14) Tian, C.; Ji, N.; Waychunas, G. A.; Shen, Y. R. Interfacial structures of acidic and basic aqueous solutions. *J. Am. Chem. Soc.* **2008**, *130* (39), 13033−13039.

(15) Levering, L. M.; Sierra-Hernandez, M. R.; Allen, H. C. Observation of hydronium ions at the air - Aqueous acid interface: Vibrational spectroscopic studies of aqueous HCI, HBr, and HI. *J. Phys. Chem. C* **2007**, *111* (25), 8814−8826.

(16) Das, S.; Bonn, M.; Backus, E. H. G. The surface activity of the hydrated proton is substantially higher than that of hydroxide. *Angew. Chem., Int. Ed.* **2019**, *58* (44), 15636−15639.

(17) Petersen, M. K.; Iyengar, S. S.; Day, T. J. F.; Voth, G. A. The Hydrated Proton at the Water Liquid/Vapor Interface. *J. Phys. Chem. B* **2004**, *108* (39), 14804−14806.

(18) Giberti, F.; Hassanali, A. A. The excess proton at the air-water interface: The role of instantaneous liquid interfaces. *J. Chem. Phys.* **2017**, *146* (24), 244703.

(19) Mucha, M.; Frigato, T.; Levering, L. M.; Allen, H. C.; Tobias, D. J.; Dang, L. X.; Jungwirth, P. Unified molecular picture of the surfaces of aqueous acid, base, and salt solutions. *J. Phys. Chem. B* **2005**, *109* (16), 7617−7623.

(20) Iuchi, S.; Chen, H.; Paesani, F.; Voth, G. A. Hydrated Excess Proton at Water−Hydrophobic Interfaces. *J. Phys. Chem. B* **2009**, *113* (13), 4017−4030.

(21) Baer, M. D.; Kuo, I.-F. W.; Tobias, D. J.; Mundy, C. J. Toward a unified picture of the water self-ions at the air−water interface: A

DOI: 10.1021/jacs.9b10807
J. Am. Chem. Soc. 2020, 142, 945−952

density functional theory perspective. *J. Phys. Chem. B* **2014**, *118* (28), 8364−8372.
(22) Tse, Y.-L. S.; Chen, C.; Lindberg, G. E.; Kumar, R.; Voth, G. A. Propensity of Hydrated Excess Protons and Hydroxide Anions for the Air−Water Interface. *J. Am. Chem. Soc.* **2015**, *137* (39), 12610−12616.
(23) Iuchi, S.; Chen, H.; Paesani, F.; Voth, G. A. Hydrated excess proton at water− hydrophobic interfaces. *J. Phys. Chem. B* **2009**, *113* (13), 4017−4030.
(24) Buch, V.; Milet, A.; Vácha, R.; Jungwirth, P.; Devlin, J. P. Water surface is acidic. *Proc. Natl. Acad. Sci. U. S. A.* **2007**, *104* (18), 7342−7347.
(25) Duignan, T. T.; Parsons, D. F.; Ninham, B. W. Hydronium and hydroxide at the air−water interface with a continuum solvent model. *Chem. Phys. Lett.* **2015**, *635*, 1−12.
(26) Jagoda-Cwiklik, B.; Cwiklik, L.; Jungwirth, P. Behavior of the Eigen form of hydronium at the air/water interface. *J. Phys. Chem. A* **2011**, *115* (23), 5881−5886.
(27) dos Santos, A. P.; Levin, Y. Surface tensions and surface potentials of acid solutions. *J. Chem. Phys.* **2010**, *133* (15), 154107.
(28) Schaefer, J.; Backus, E. H. G.; Nagata, Y.; Bonn, M. Both Inter- and Intramolecular Coupling of O−H Groups Determine the Vibrational Response of the Water/Air Interface. *J. Phys. Chem. Lett.* **2016**, *7* (22), 4591−4595.
(29) Sengupta, S.; Moberg, D. R.; Paesani, F.; Tyrode, E. Neat Water−Vapor Interface: Proton Continuum and the Nonresonant Background. *J. Phys. Chem. Lett.* **2018**, *9* (23), 6744−6749.
(30) Vinaykin, M.; Benderskii, A. V. Vibrational Sum-Frequency Spectrum of the Water Bend at the Air/Water Interface. *J. Phys. Chem. Lett.* **2012**, *3* (22), 3348−3352.
(31) Nagata, Y.; Hsieh, C. S.; Hasegawa, T.; Voll, J.; Backus, E. H. G.; Bonn, M. Water Bending Mode at the Water-Vapor Interface Probed by Sum-Frequency Generation Spectroscopy: A Combined Molecular Dynamics Simulation and Experimental Study. *J. Phys. Chem. Lett.* **2013**, *4* (11), 1872−1877.
(32) Kundu, A.; Tanaka, S.; Ishiyama, T.; Ahmed, M.; Inoue, K.-i.; Nihonyanagi, S.; Sawai, H.; Yamaguchi, S.; Morita, A.; Tahara, T. Bend Vibration of Surface Water Investigated by Heterodyne-Detected Sum Frequency Generation and Theoretical Study: Dominant Role of Quadrupole. *J. Phys. Chem. Lett.* **2016**, *7* (13), 2597−2601.
(33) Liu, D.; Ma, G.; Levering, L. M.; Allen, H. C. Vibrational spectroscopy of aqueous sodium halide solutions and air− liquid interfaces: Observation of increased interfacial depth. *J. Phys. Chem. B* **2004**, *108* (7), 2252−2260.
(34) Wen, Y. C.; Zha, S.; Liu, X.; Yang, S. S.; Guo, P.; Shi, G. S.; Fang, H. P.; Shen, Y. R.; Tian, C. S. Unveiling Microscopic Structures of Charged Water Interfaces by Surface-Specific Vibrational Spectroscopy. *Phys. Rev. Lett.* **2017**, *116*, 016101.
(35) Stiopkin, I. V.; Jayathilake, H. D.; Bordenyuk, A. N.; Benderskii, A. V. Heterodyne-detected vibrational sum frequency generation spectroscopy. *J. Am. Chem. Soc.* **2008**, *130* (7), 2271−2275.
(36) Nihonyanagi, S.; Yamaguchi, S.; Tahara, T. Direct evidence for orientational flip-flop of water molecules at charged interfaces: A heterodyne-detected vibrational sum frequency generation study. *J. Chem. Phys.* **2009**, *130* (20), 204704.
(37) Marx, D.; Tuckerman, M. E.; Hutter, J.; Parrinello, M. The nature of the hydrated excess proton in water. *Nature* **1999**, *397* (6720), 601−604.
(38) Knight, C.; Voth, G. A. The curious case of the hydrated proton. *Acc. Chem. Res.* **2012**, *45* (1), 101−109.
(39) Tyrode, E.; Sengupta, S.; Sthoer, A. *Identifying Eigen-Like Hydrated Protons at Negatively Charged Interfaces*. DOI: 10.26434/chemrxiv.9701468.v1.
(40) Yu, Q.; Carpenter, W. B.; Lewis, N. H.; Tokmakoff, A.; Bowman, J. M. High-Level VSCF/VCI Calculations Decode the Vibrational Spectrum of the Aqueous Proton. *J. Phys. Chem. B* **2019**, *123* (33), 7214−7224.
(41) Ceriotti, M.; Fang, W.; Kusalik, P. G.; McKenzie, R. H.; Michaelides, A.; Morales, M. A.; Markland, T. E. Nuclear quantum effects in water and aqueous systems: Experiment, theory, and current challenges. *Chem. Rev.* **2016**, *116* (13), 7529−7550.
(42) Vacha, R.; Buch, V.; Milet, A.; Devlin, P.; Jungwirth, P. Autoionization at the surface of neat water: is the top layer pH neutral, basic, or acidic? *Phys. Chem. Chem. Phys.* **2007**, *9* (34), 4736−4747.
(43) Lee, H.-S.; Tuckerman, M. E. Ab Initio Molecular Dynamics Studies of the Liquid−Vapor Interface of an HCl Solution. *J. Phys. Chem. A* **2009**, *113* (10), 2144−2151.
(44) Wei, X.; Shen, Y. R. Motional effect in surface sum-frequency vibrational spectroscopy. *Phys. Rev. Lett.* **2001**, *86* (21), 4799.
(45) Gan, W.; Wu, D.; Zhang, Z.; Feng, R.-r.; Wang, H.-f. Polarization and experimental configuration analyses of sum frequency generation vibrational spectra, structure, and orientational motion of the air/water interface. *J. Chem. Phys.* **2006**, *124* (11), 114705.
(46) Sun, S.; Tang, F.; Imoto, S.; Moberg, D. R.; Ohto, T.; Paesani, F.; Bonn, M.; Backus, E. H. G.; Nagata, Y. Orientational distribution of free OH groups of interfacial water is exponential. *Phys. Rev. Lett.* **2018**, *121* (24), 246101.
(47) Petersen, P. B.; Saykally, R. J. Probing the Interfacial Structure of Aqueous Electrolytes with Femtosecond Second Harmonic Generation Spectroscopy. *J. Phys. Chem. B* **2006**, *110* (29), 14060−14073.
(48) Willard, A. P.; Chandler, D. Instantaneous liquid interfaces. *J. Phys. Chem. B* **2010**, *114* (5), 1954−1958.
(49) Wick, C. D. Comparing hydroxide and hydronium at the instantaneous air-water interface using polarizable multi-state empirical valence bond models. *Comput. Theor. Chem.* **2017**, *1116*, 64−72.
(50) Stern, A. C.; Baer, M. D.; Mundy, C. J.; Tobias, D. J. Thermodynamics of iodide adsorption at the instantaneous air-water interface. *J. Chem. Phys.* **2013**, *138* (11), 114709.
(51) Tang, F.; Ohto, T.; Hasegawa, T.; Xie, W. J.; Xu, L.; Bonn, M.; Nagata, Y. Definition of free O−H groups of water at the air−water interface. *J. Chem. Theory Comput.* **2018**, *14* (1), 357−364.
(52) Sedlmeier, F.; Horinek, D.; Netz, R. R. Nanoroughness, intrinsic density profile, and rigidity of the air-water interface. *Phys. Rev. Lett.* **2009**, *103* (13), 136102.
(53) Baer, M. D.; Fulton, J. L.; Balasubramanian, M.; Schenter, G. K.; Mundy, C. J. Persistent ion pairing in aqueous hydrochloric acid. *J. Phys. Chem. B* **2014**, *118* (26), 7211−7220.
(54) Baer, M. D.; Tobias, D. J.; Mundy, C. J. Investigation of interfacial and bulk dissociation of HBr, HCl, and HNO_3 using density functional theory-based molecular dynamics simulations. *J. Phys. Chem. C* **2014**, *118* (50), 29412−29420.
(55) Napoli, J. A.; Marsalek, O.; Markland, T. E. Decoding the spectroscopic features and time scales of aqueous proton defects. *J. Chem. Phys.* **2018**, *148* (22), 222833.
(56) Dreier, L. B.; Wolde-Kidan, A.; Bonthuis, D. J.; Netz, R. R.; Backus, E. H. G.; Bonn, M. Unraveling the origin of the apparent charge of zwitterionic lipid layers. *J. Phys. Chem. Lett.* **2019**, *10* (20), 6355−6359.
(57) VandeVondele, J.; Krack, M.; Mohamed, F.; Parrinello, M.; Chassaing, T.; Hutter, J. Quickstep: Fast and accurate density functional calculations using a mixed Gaussian and plane waves approach. *Comput. Phys. Commun.* **2005**, *167* (2), 103−128.
(58) Zhang, Y.; Yang, W. Comment on "Generalized gradient approximation made simple. *Phys. Rev. Lett.* **1998**, *80* (4), 890.
(59) Grimme, S.; Antony, J.; Ehrlich, S.; Krieg, H. A consistent and accurate ab initio parametrization of density functional dispersion correction (DFT-D) for the 94 elements H-Pu. *J. Chem. Phys.* **2010**, *132* (15), 154104.
(60) Ohto, T.; Dodia, M.; Xu, J.; Imoto, S.; Tang, F.; Zysk, F.; Kuehne, T. D.; Shigeta, Y.; Bonn, M.; Wu, X. Accessing the Accuracy of Density Functional Theory through Structure and Dynamics of the Water− Air Interface. *J. Phys. Chem. Lett.* **2019**, *10* (17), 4914−4949.

DOI: 10.1021/jacs.9b10807
J. Am. Chem. Soc. 2020, 142, 945−952

(61) Morita, A.; Hynes, J. T. A theoretical analysis of the sum frequency generation spectrum of the water surface. *Chem. Phys.* **2000**, *258* (2−3), 371−390.
(62) Neese, F. The ORCA program system. *Wiley Interdiscip. Rev. Comput. Mol. Sci.* **2012**, *2* (1), 73−78.

DOI: 10.1021/jacs.9b10807
J. Am. Chem. Soc. 2020, 142, 945−952